CHAPTER IV

SOLUTION PROCEDURE OF OPTIMAL POWER FLOW

4.1 Introduction

The formulation of optimal power flow (OPF) is firstly introduced in this chapter. Then, the sequential and the parallel of SADE_ALM for solving the OPF problems are presented, followed by numerical results and discussion. Conclusion is provided in the last section.

4.2 Optimal Power Flow (OPF) Problem Formulation

The optimal power flow (OPF) problem is to minimize the total generator fuel cost function subject to power balance constraints and inequality constraints imposed on the operation of power system. Mathematically, the OPF problem can be formulated as follows:

$$Min\ J(X,U) \tag{4.1}$$

subject to

$$h(X,U)=0 \tag{4.2}$$

$$g(X,U)\le 0 \tag{4.3}$$

where U is the vector of state variables consisting of real power of slack generator P_{G_1}, voltage magnitude of load buses V_L, reactive power of all generators Q_G, transformer and transmission line loadings S_l. Therefore, U can be expressed as $U^T=[P_{G_1},V_{L_1},\ldots,V_{L_{NL}},Q_{G_1},\ldots,Q_{G_{NG}},S_{l_1},\ldots,S_{l_{NBR}}]$ where NL, NG, and NBR are number of load buses, number of generators, and number of transformers and transmission lines.

X is the vector of control variables consisting of real power of all generators excluding slack generator, voltage magnitude of all generators V_G, and transformer tap settings T. Therefore, X can be expressed as $X^T=[P_{G_2},\ldots,P_{G_{NG}},V_{G_1},\ldots,V_{G_{NG}},T_1,\ldots,T_{NT}]$ where NT is the number of regulating transformers.

$J(X,U)$ is the objective function to be minimized. Generally, in the OPF problem, the objective function J is the total generator fuel cost, i.e.

$$J=\sum_{i=1}^{NG} f_i\left(P_{G_i}\right) \tag{4.4}$$

where $f_i\left(P_{G_i}\right)$ is the fuel cost function of the ith generator.

$h(X,U)$ is the equality constraints and represent typical power flow equations.

$g(X,U)$ is the system operating constraints.

The system operating constraints can be described below.

1) Generation constraints: Real and reactive power outputs, and voltage magnitude of generators are restricted by the lower and upper limits, i.e.

$$V_{G_i}^{\min} \le V_{G_i} \le V_{G_i}^{\max}, \qquad i \in NG \tag{4.5}$$

$$P_{G_i}^{\min} \le P_{G_i} \le P_{G_i}^{\max}, \qquad i \in NG \tag{4.6}$$

$$Q_{G_i}^{\min} \le Q_{G_i} \le Q_{G_i}^{\max}, \qquad i \in NG \tag{4.7}$$

2) Ramp-rate constraints: The ramp-rate constraint restricts the operating range of the physical lower and upper limit to the effective lower limit $P_{G_i}^{\min(R)}$ and upper limit $P_{G_i}^{\max(R)}$ respectively [62]. These limits can be defined as

$$P_{G_i}^{min(R)} = max[P_{G_i}^{min}, P_{G_i}^{0} - DR_i] \tag{4.8}$$

$$P_{G_i}^{max(R)} = min[P_{G_i}^{max}, P_{G_i}^{0} + UR_i] \tag{4.9}$$

where $P_{G_i}^{0}$ is the power generation of ith unit at previous hour, and DR_i and UR_i are the decreasing and increasing ramp-rate limits of ith unit respectively. Therefore, the ramp rate constraint can be defined as

$$P_{G_i}^{min(R)} \le P_{G_i} \le P_{G_i}^{max(R)} \tag{4.10}$$

3) Transformer constraints: Transformer tap settings are restricted by the lower and upper limits as follows:

$$T_i^{min} \le T_i \le T_i^{max}, \qquad i \in NT \tag{4.11}$$

4) Securities constraints: These include the constraints of voltage magnitude at load buses and power flow through transformers and transmission line (MVA loading) as follows:

$$V_{L_i}^{min} \le V_{L_i} \le V_{L_i}^{max}, \qquad i \in NL \tag{4.12}$$

$$S_{l_i} \le S_{l_i}^{max}, \qquad i \in NBR \tag{4.13}$$

Four cases of the generator fuel cost function are used to verify the ability and robustness of the proposed algorithms to solve the OPF problems, They are listed below.

1) Quadratic cost curve model,

2) Piecewise quadratic cost curve model (multiple fuels),

3) Quadratic cost curve with rectified sine component model (valve-point effects), and

4) Combined multiple fuels, valve-point effects, and combined cycle cogeneration plant (CCCP) model.

The conventional quadratic fuel cost function, the piecewise quadratic cost function, and the quadratic cost function with rectified sine component are given by (3.1), (3.2), and (3.3) in chapter 3 respectively.

For combined cycle co-generation plant, the fuel cost characteristic of the CCCP is also non-smooth and non-differentiable form. In CCCP, gas and steam turbines are working in combination to generate electric power. Specifically, if the configuration of the CCCP is a topping cycle, the steam turbines can generate electric power from the wasted heat of gas turbine units [63]. Figure 4.1 shows an example of the fuel cost curve of a CCCP with two gas turbines and one steam turbine where mathematical description of the fuel cost function can be simplified as follows [3]:

$$f_i(P_{G_i}) = \begin{cases} b_i P_{G_i} + c_i, & \textit{linear region (\$/hr.)} \\ K, & \textit{constant region (\$/hr.)} \end{cases} \tag{4.14}$$

where b_i and c_i are cost coefficients of CCCP in linear region and K is the cost coefficient of CCCP in constant region.

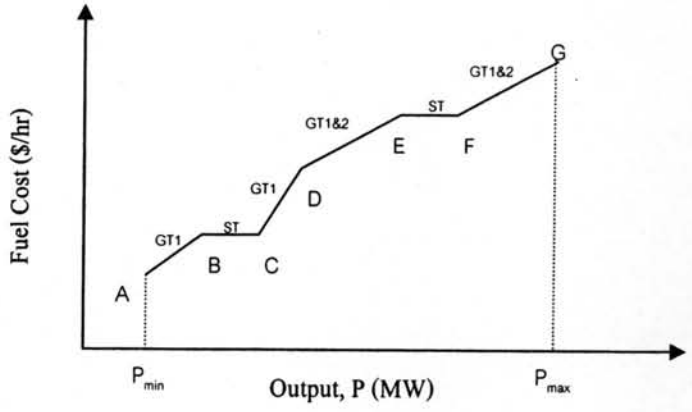

GT1, GT2: Gas Turbine Generator Unit No. 1&2, ST: Steam Turbine Generator

Figure 4.1 Fuel-cost characteristic of CCCP with two gas turbines and one steam turbine

The regions of B-C and E-F shown in the Figure 4.1 are produced from the steam turbine which is driven from the exhausted heat of the gas turbines; thereby no additional fuel costs are required in these regions.

It is worth mentioning that the inequality constraints of the control variables are self-constrained. In this paper, the inequality constraints of the state variables are handled using the augmented lagrange multiplier (ALM) method. Generally, the penalty function is the most popular method for handling inequality constraints, due to its simple concept and convenience to implementation. However, the penalty function method does suffer from the complication that as the penalty parameter is increased toward infinity; the structure of the unconstrained problem becomes increasing ill-conditioned. Therefore, each unconstrained minimization problem becomes more difficult to solve, which has the effect of slowing the convergence rate of the overall optimization process. On the other hand, if the penalty parameters are too small, the constraint violation will not impose a high cost on the penalty function. Thus the optimal solution based on the penalty function may not be feasible, whereas the ALM method can be employed easily to handle inequality constraints without those difficulties as already described in chapter 2.

The unconstrained minimization problem through the augmented lagrange function L_a can be defined by augmented the m-inequality constraints of the state variables with the objective function as shown below [1, 2].

$$L_a = f(X,U) + r_g \sum_{j=1}^{m} \left\{ max\left[g_j(X,U), -\frac{\beta_j}{2r_g} \right] \right\}^2 + \sum_{j=1}^{m} \beta_j \left\{ max\left[g_j(X,U), -\frac{\beta_j}{2r_g} \right] \right\} \tag{4.15}$$

where $g_j(\cdot)$, j = 1,2,..., m, m = 2(1+NL+NG)+NBR are the m-inequality constraints of the state variables which can be defined as follows:

1) Real power of slack generator,

$$g_1 = \left(-P_{G_1} + P_{G_1}^{\min} \right) \tag{4.16}$$

$$g_2 = \left(P_{G_1} - P_{G_1}^{\max} \right) \tag{4.17}$$

2) Voltage magnitude of load buses V_{L_i}, $i = 1,\ldots, NL$

$$g_i = \left(-V_{L_i} + V_{L_i}^{\min}\right) \tag{4.18}$$

$$g_{i+1} = \left(V_{L_i} - V_{L_i}^{\max}\right) \tag{4.19}$$

3) Reactive power of generators Q_{G_i}, $i = 1,\ldots, NG$

$$g_i = \left(-Q_{G_i} + Q_{G_i}^{\min}\right) \tag{4.20}$$

$$g_{i+1} = \left(Q_{G_i} - Q_{G_i}^{\max}\right) \tag{4.21}$$

4) Transformer and transmission line loadings S_{l_i}, $i = 1,\ldots, NBR$

$$g_i = \left(S_{l_i} - S_{l_i}^{\max}\right) \tag{4.22}$$

r_g is the positive penalty multiplier, and

β_js are the lagrange multipliers of the associated inequality constraints.

After the unconstrained minimization problem has been solved, the lagrange multipliers β_js and the penalty parameter r_g will be updated to create the new augmented lagrange function L_a as follows [1, 2]:

$$\beta_j^{i+1} = \beta_j^i + 2r_g \left\{ max\left[g_j(X,U), -\frac{\beta_j^i}{2r_g} \right] \right\} \tag{4.23}$$

$$r_g^{i+1} = \begin{cases} c_g \times r_g^i, & if\ r_g^i \le r_{g,max} \\ r_{g,max}, & otherwise \end{cases} \tag{4.24}$$

where c_g is the positive constant increasing rate, and $r_{g,max}$ is the maximum penalty multiplier.

From (4.23), it can be seen that the lagrange multipliers β_js are deterministically updated using the inequality constraint functions evaluated from the previous solution of the unconstrained minimization problem, while the penalty parameter r_g is increased by a constant rate until it reaches the predetermined maximum value as shown in (4.24). The algorithm is then repeated until termination. The detail of the proposed algorithms will be described in the next section.

4.3 SADE_ALM Based Optimal Power Flow (SADE_ALM-OPF)

The proposed self-adaptive differential evolution with augmented lagrange multiplier method (SADE_ALM) for solving the OPF problems consists of two iterative loops, i.e. the inner and the outer loops. The inner loop solves the unconstrained minimization problem through the augmented lagrange function L_a using self-adaptive differential evolution (SADE). After the unconstrained minimization problem has been solved, the outer loop will update the lagrange multipliers βs and the penalty parameter r_g by the ALM method to create the new augmented lagrange function L_a. The algorithm is then repeated until a termination criterion, i.e. maximum number of iterations or convergence of the optimal solution, is reached. The flowchart of the SADE_ALM when applied to solve the OPF problems is shown in Figure 4.2. Details of the proposed algorithm can be summarized hereafter.

4.3.1 The inner loop iteration

The details of the outer loop can be described as shown below.

1) Initialization

Set maximum iteration number of the inner loop (N_i), convergence tolerance ($\varepsilon_{\Delta X}$), and then create the initial population size, NP, associated with their lower and upper limits as follows:

$$x_{ij} = x_{ij,low} + \rho_{ij} \times \left(x_{ij,hi} - x_{ij,low}\right) \tag{4.25}$$

$$F_j = F_{j,low} + \rho_{1j} \times \left(F_{j,hi} - F_{j,low}\right) \tag{4.26}$$

$$CR_j = CR_{j,low} + \rho_{2j} \times \left(CR_{j,hi} - CR_{j,low}\right) \tag{4.27}$$

where

x_{ij} is the OPF control variable i of the n-dimensional parent vector X_j,

$x_{ij,low}$, and $x_{ij,hi}$ are the lower and upper limits of x_{ij}

F_j is the mutation factor for individual X_j,

$F_{j,low}$, and $F_{j,hi}$ are the lower and upper limits of F_j,

CR_j is the crossover constant for individual X_j,

$CR_{j,low}$, and $CR_{j,hi}$ are the lower and upper limits of CR_j, and

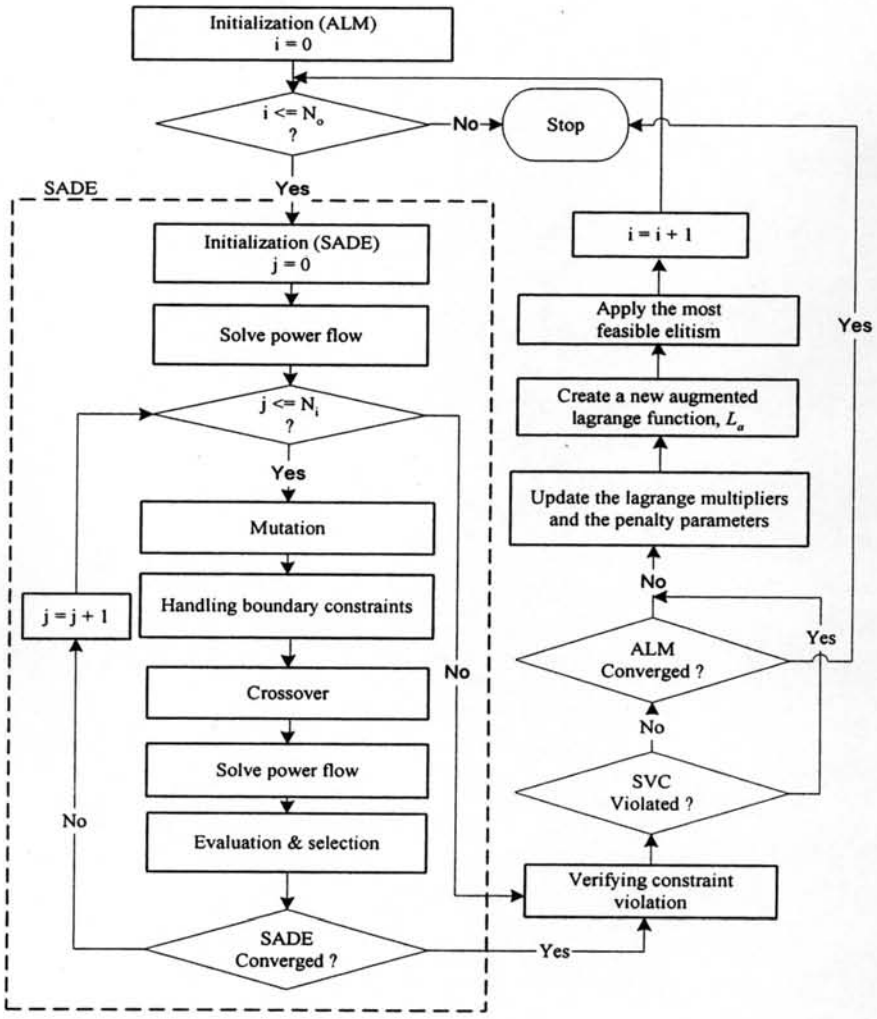

Figure 4.2 Flowchart of SADE_ALM-OPF

ρ_{ij}, ρ_{1j}, and ρ_{2j} are uniformly distributed random numbers within [0,1] for individual x_{ij}, F_j, and CR_j respectively.

An individual X_j in a population represents a candidate of OPF solution. Each individual consists of F_j, CR_j, and OPF control variables x_{ij} including real power of all generators excluding slack generator, voltage magnitude of all generators including slack generator, and transformer tap settings. For generators considering ramp rate constraints, the operating range of the physical lower and upper limit will be restricted to the effective lower and upper limit according to (4.8) and (4.9) respectively.

2) Power flow solution

For each individual X_j, the Newton-Raphson (NR) power flow is applied to determine the state variables of the associated X_j. If the power flow of any individuals fails to converge, such individuals will be removed and replaced by new randomly generated individuals. This process is repeated until the power flow calculations of such individuals are converged.

3) Mutation

For each individual X_j, a mutant vector X'_j is created according to the following expression.

$$x'_{ij} = x_{ij,r_3} + F_j \times \left(x_{ij,r_1} - x_{ij,r_2}\right) \tag{4.28}$$

$$F'_j = F_{j,r_3} + F_j \times \left(F_{j,r_1} - F_{j,r_2}\right) \tag{4.29}$$

$$CR'_j = CR_{j,r_3} + F_j \times \left(CR_{j,r_1} - CR_{j,r_2}\right) \tag{4.30}$$

where r_1, r_2, and r_3 are randomly chosen indices such that r_1, r_2, and $r_3 \in (1,NP)$ and $r_1 \neq r_2 \neq r_3 \neq j$.

4) Handling boundary constraints

In the event that mutation causes control variables, x'_{ij}, F'_j, and CR'_j, exceeded their boundary constraints, i.e. lower or upper limit, such variables will be set to the nearest boundary.

5) Crossover

To increase the diversity of the mutant vectors, crossover is introduced to create the trial vector X''_j based on a series of n-1 binomial experiments [17] as follows:

$$x''_{ij} = \begin{cases} x'_{ij}, \forall \rho_{ij} \leq CR_j \ \ or \ \ i = i_{rand} \\ x_{ij}, otherwise \end{cases} \tag{4.31}$$

$$F''_j = \begin{cases} F'_j, \forall \rho_{1j} \leq CR_j \ \ or \ \ i_{rand} = 1 \\ F_j, otherwise \end{cases} \tag{4.32}$$

$$CR''_j = \begin{cases} CR'_j, \forall \rho_{2j} \leq CR_j \ \ or \ \ i_{rand} = 2 \\ CR_j, otherwise \end{cases} \tag{4.33}$$

where ρ_{ij}, ρ_{1j}, and ρ_{2j} are the uniformly distributed random number within [0,1] for individual x''_{ij}, F''_j, and CR''_j respectively, and $i_{rand} \in (1, n+2)$ is a generated random integer number to ensure that the trial vector X''_j is different from its associated parent vector X_j.

6) Evaluation and selection

To create the new population in the next generation G+1, the fitness value or the augmented objective value in (4.15) of the trial vector $X_j^{\pi(G)}$ is compared with its parent vector $X_j^{(G)}$ in the same way as in the classical DE as shown below.

$$X_j^{(G+1)} = \begin{cases} X_j^{\pi(G)}, \ if \ L_a\left(X_j^{\pi(G)}\right) \le L_a\left(X_j^{(G)}\right) \\ X_j^{(G)}, \ otherwise \end{cases} \tag{4.34}$$

The inner loop will be terminated according to two defined criteria, i.e. 1) maximum iteration number of the inner loop (N_i), and 2) convergence of the optimal solution as follows:

$$\Delta X_{opt} \le \varepsilon_{\Delta X} \tag{4.35}$$

where $\varepsilon_{\Delta X}$ is a convergence tolerance value of ΔX_{opt}, determined by

$$\Delta X_{opt} = \left\| X_{opt}^{(G)} - X_{opt}^{(G-1)} \right\|_{\infty} \tag{4.36}$$

where $\| . \|_{\infty}$ is the infinity-norm, $X_{opt}^{(G)}$ and $X_{opt}^{(G-1)}$ are the optimal solution obtained at current generation (G) and previous generation (G-1) respectively.

4.3.2 The outer loop iteration

After the inner loop has converged, the outer loop is started by using the ALM method to handle the inequality constraints of the state variables. The details of the outer loop can be described as shown below.

1) Initialization

Set maximum iteration of the outer loop (N_o), the constrain violation tolerance (ε_{SVC}), the lagrange multiplier βs, and the penalty parameters r_g including c_g, and $r_{g.max}$.

2) Verifying constrain violation

The constrain violation of the optimal solution obtained from the inner loop ($X_{opt}^{\bullet}$) is verified through the sum of the violated constraints (SVC) index as shown in (4.37) and (4.38).

$$SVC \le \varepsilon_{SVC} \tag{4.37}$$

$$SVC = \sum_{j=1}^{m} \left\{ max \left[g_j\left(X_{opt}^{\bullet}\right), 0 \right] \right\} \tag{4.38}$$

where $g_j(\cdot)$, j = 1,2,..., m are the m-inequality constraints of the state variables as explained in section 2.

3) Creating a new unconstrained minimization problem

To create a new unconstrained minimization problem for the next inner loop iteration, the new augmented lagrange function L_a is created by updating the lagrange multiplier βs and the penalty parameter r_g according to (4.23), and (4.24) respectively.

4) Appling the most feasible elitism

To improve the efficiency of the proposed algorithm, the most feasible elitism (X_{elite}) is employed by replacing the worst individual X_j which has the highest fitness value for the next inner loop iteration. The elitist member is initialized by using the optimal solution obtained from the first inner loop iteration. Then, it is updated according to the extent of the violated SVC value and the total generator fuel cost in (4.4) as follows:

1) If $SVC\left(X_{elite}^{(K-1)}\right) > \varepsilon_{SVC}$, then

$$X_{elite}^{(K)} = \begin{cases} X_{opt}^{*(K)}, \ if \ SVC\left(X_{opt}^{*(K)}\right) \le SVC\left(X_{elite}^{(K-1)}\right) \\ \qquad and \ J\left(X_{opt}^{*(K)}\right) \le J\left(X_{elite}^{(K-1)}\right) \\ X_{elite}^{(K-1)}, \ otherwise \end{cases} \tag{4.39}$$

2) If $SVC\left(X_{elite}^{(K-1)}\right) \le \varepsilon_{SVC}$, then

$$X_{elite}^{(K)} = \begin{cases} X_{opt}^{*(K)}, \ if \ J\left(X_{opt}^{*(K)}\right) \le J\left(X_{elite}^{(K-1)}\right) \\ X_{elite}^{(K-1)}, \ otherwise \end{cases} \tag{4.40}$$

where $X_{elite}^{(K)}$ and $X_{elite}^{(K-1)}$ are the elitist members of the current (K) and previous (K-1) iteration of the outer loop respectively, and $X_{opt}^{*(K)}$ is the optimal solution obtained from the current (K) iteration of the inner loop.

The outer loop will be terminated according to the same criteria as defined for the inner loop, i.e. 1) maximum iteration number of the outer loop (N_o), and 2) convergence of the optimal solution.

4.4 Parallel SADE_ALM Based Optimal Power Flow (pSADE_ALM-OPF)

The proposed pSADE_ALM is a modified version of sequential self-adaptive differential evolution (SADE_ALM) [1, 2] by exploiting parallel processing techniques to increase the search capability of the algorithm via PC cluster. Due to our limited resources, the PC cluster consists of

3x2.8 GHz Pentium IV processors arranged in master-slave structure with 256 MB RAM for each PC, 1x4 ports KVM switch, and 1x8 ports 10/100 Fast Ethernet Switching as shown in Figure 4.3. The program was developed based on free numerical software SCILAB 4.0 [61] running on LINUX Fedora Core 2, and the message passing interface employed a PVM parallel toolbox from SCILAB. The PVM [64] is a software package that permits heterogeneous computers hooked together by a network and used as a single large parallel computer. Therefore, large computational problems can be solved more cost effectively by using the aggregated power and memory of many computers. An overview of parallel evolutionary algorithms is described in Appendix C.

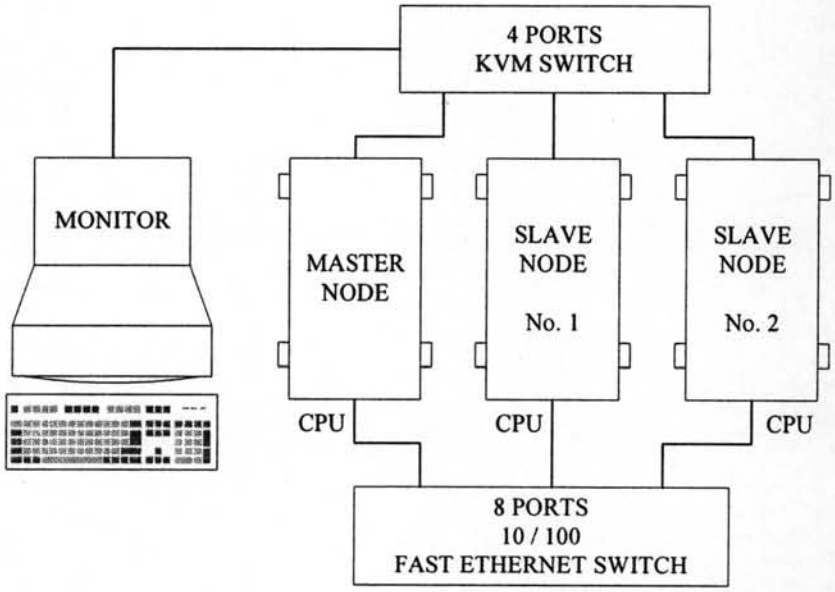

Figure 4.3 Structure of PC cluster

The proposed pSADE_ALM consists of two iterative loops, i.e. the inner loop and the outer loop. The inner loop iteration is implemented independently by all PCs with different DE's strategies [20]. As in section 2.3 of chapter 2, typical DE's strategies are classified using the following notation: DE/x/y/z, where x indicates the method for selecting the parent chromosome or the parent vector that will form the base of the mutant vector, y indicates the number of different vectors used to perturb the base of the mutant vector, and z indicates the recombination or the crossover mechanism used to create the offspring or the trial vector that already described in chapter 2. For our proposed method, three different DE's strategies, i.e. DE/rand/1/bin, DE/rand-to-best/1/bin, and DE/best/2/bin are assigned to slave node 1, slave node2, and master

node respectively. Details of these strategies are described in Appendix A. For each PC, the inner loop iteration solves the unconstrained minimization problem through the augmented lagrange function L_a using self-adaptive differential evolution (SADE) [1, 2]. After the unconstrained minimization problem has been solved independently by all PCs, the master node will implement the outer loop iteration. Firstly, the master node will compare and determine the best optimal result from all PCs based on the extent of the constraint violation and the total generator fuel cost. Then, the master node will update the lagrange multipliers βs and the penalty parameter r_g to create the new augmented lagrange function $L_{a'}$. The algorithm is then repeated until a termination criterion, i.e. maximum number of iterations or convergence of the optimal solution, is reached. The flowchart of the pSADE_ALM when applied to solve the OPF problems is shown in Figure 4.4.

4.4.1 The inner loop iteration

For each PC, the inner loop solves the augmented lagrange function L_a using self-adaptive differential evolution (SADE) based on its DE's strategy. The algorithm of the inner loop iteration of pSADE_ALM is similar to SADE_ALM as described in section 4.3.1.

4.4.2 The outer loop iteration

After all PCs have finished the inner loop iteration, the master node starts the outer loop iteration by using the ALM method to handle the inequality constraints of the state variables. The details of the outer loop can be described as shown below.

1) Initialization

Set maximum iteration of the outer loop (N_o), the constrain violation tolerance (ε_{SVC}), the lagrange multiplier βs, and the penalty parameters r_g including c_g, and $r_{g,max}$.

2) Determined the best optimal inner loop iteration

The master node will determine the best optimal inner loop iteration (X^*_{opt}) by comparing the final result of all PCs based on the sum of the violated constraints (*SVC*) index in (4.37) and (4.38) and the total generator fuel cost in (4.4).

3) Checking constrain violation

The constrain violation of the best optimal inner loop iteration (X^*_{opt}) is checked through the sum of the violated constraints (*SVC*) index as shown in (4.37) and (4.38).

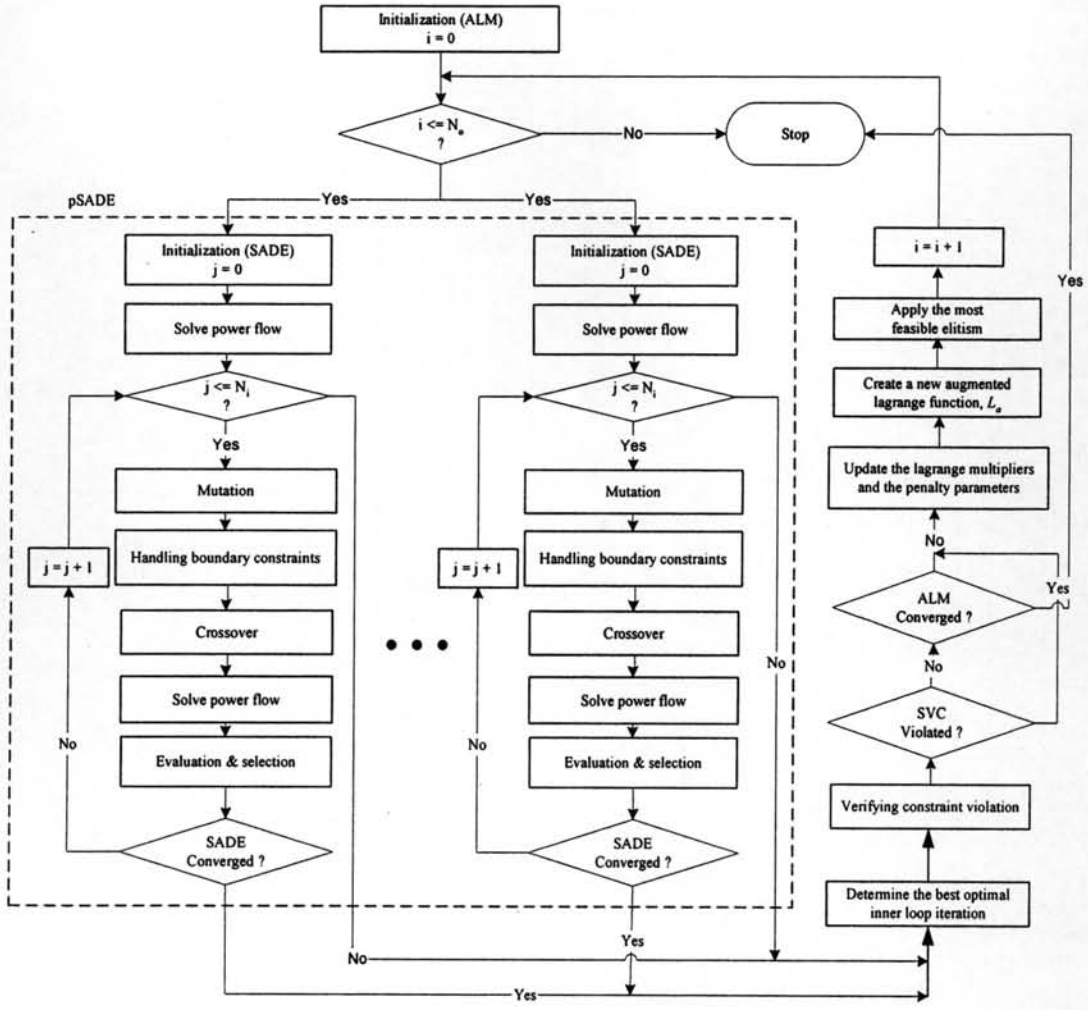

Figure 4.4 Flowchart of pSADE_ALM-OPF

4) Creating the new unconstrained minimization problem

The new unconstrained minimization problem through the new augmented lagrange function L_a is created by updating the lagrange multiplier βs and the penalty parameter r_g according to (4.23), and (4.24) respectively.

5) Appling the most feasible elitism

To improve the efficiency of the proposed algorithm, the most feasible elitism (X_{elite}) is employed by replacing the worst individual X_j which has the highest fitness value for the next inner loop iteration. The elitist member is initialized by using the optimal solution obtained from the first inner loop iteration. Then, it is updated according to the extent of the sum of the violated constraints (*SVC*) index in (4.37) and (4.38) and the total generator fuel cost in (4.4). The outer

loop will be terminated according to the same criteria as the inner loop, i.e. 1) maximum iteration number of the outer loop (N_o), and 2) convergence of the optimal solution.

4.5 Numerical Results

Both SADE_ALM and pSADE_ALM were implemented to solve the OPF problems based on the IEEE-30 bus system given in O. Alsac and B. Stott [65] of which the bus, generator, and branch data are presented in Table D.1-D.3 in Appendix D respectively. The effectiveness of both algorithms has been tested and compared with other approaches, i.e. TS [9], TS/SA [10], ITS [11], EP [7, 12, 13], IEP [14], and parallel EP [24] based on different fuel cost characteristics, i.e. 1) quadratic cost curve model, 2) piecewise quadratic cost curve model (multiple fuels), 3) quadratic cost curve with rectified sine component model (valve-point effects), and 4) combined multiple fuels, valve-point effects, and combined cycle cogeneration plant (CCCP) model. In addition, the OPF problems with quadratic fuel cost function for the IEEE 57 and 118 bus system [66] were also implemented. The bus, generator, and branch data for the IEEE 57 and 118 bus system are presented in Appendix E and F respectively. The in-phase transformers for both test systems were assumed to be adjustable tap setting in ranges of ± 10%. For each case, 10 independent runs were conducted.

The parameters of SADE_ALM and pSADE_ALM for all test cases were set as follows: NP = 20, F = [0.2, 1], CR = [0.1, 1], $r_g = 10^3$, $c_g = 100$, $r_{gmax} = 10^8$, $N_i = 10^3$, $N_o = 5$, $\varepsilon_{\Delta X} = 10^{-3}$, $\varepsilon_{SVC} = 10^{-7}$. In addition, the lagrange multiplier (βs) of inequality constraints were initialized using zeros values for all cases. The programs were developed based on free numerical software SCILAB 4.0 [61] on PC Cluster 3x2.8 GHz Pentium IV processors with 256 MB RAM for each PC as described in section 4.3.

4.5.1 Case 4.1: The OPF with Quadratic Fuel Cost Function for the IEEE 30 Bus System.

For this case, bus 1 is the slack bus of the system and the generator cost curves of all the generators are represented by quadratic function as shown in (3.1). The generator cost coefficients are given in Table 4.1 [7, 14]. The simulation results are shown in Table 4.2 and the convergence characteristic of SADE_ALM and pSADE_ALM is shown in Figure 4.5.

Table 4.1 Generator cost coefficients in case 4.1

Bus No.	Real power output limit (MW)		Cost Coefficients		
	Min	Max	a	b	c
1	50	200	0.00375	2.00	0
2	20	80	0.01750	1.75	0
5	15	50	0.06250	1.00	0
8	10	35	0.00834	3.25	0
11	10	30	0.02500	3.00	0
13	12	40	0.02500	3.00	0

Table 4.2 Comparison of the total generator fuel costs for case 4.1

Algorithm	Fuel Cost ($/hr.)				Average computational time (minutes)
	Best cost	Average cost	Worst cost	S.D. of cost	
Gradient [65]	802.40	N/A	N/A	N/A	N/A
EP [14]	802.907	803.232	803.474	0.226	66.693
TS [14]	802.502	802.632	802.746	0.080	86.227
TS/SA [14]	802.788	803.032	803.291	0.187	62.275
ITS [14]	804.556	805.812	806.856	0.754	88.495
IEP [14]	802.465	802.521	802.581	0.039	99.013
parallel EP[1)] [24]	802.510	803.330	804.280	N/A	5.020
SADE_ALM	802.404	802.407	802.411	0.003	15.934
pSADE_ALM	802.405	802.405	802.405	0.000	17.295

Notes: 1) Computational time is based on different computing hardware

2) Based on 50 different runs on 31 Intel Pentium IV 2.66 GHz processors

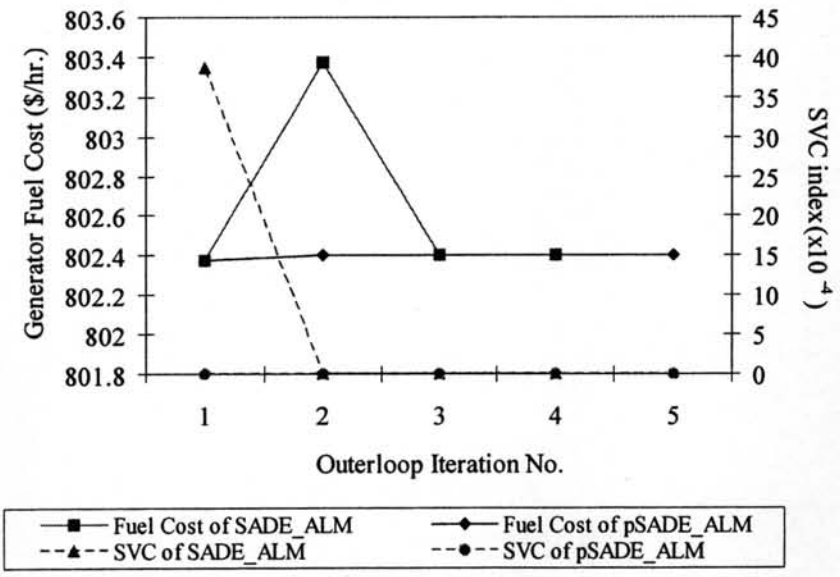

Figure 4.5 Convergence characteristic of SADE_ALM and pSADE_ALM for case 4.1

4.5.2 Case 4.2: The OPF with multiple fuels for the IEEE 30 Bus System.

In this case, the generator fuel cost curves of generator at bus 1 and 2 are represented by piecewise quadratic functions using (3.3). Bus 5 is selected as the slack bus of the system to allow more accurate control over units with discontinuities in cost curves [7]. The generator cost coefficients of those two generators are given in Table 4.3 [7, 14]. The simulation results are shown in Table 4.4 and the convergence characteristic of SADE_ALM and pSADE_ALM is shown in Figure 4.6.

Table 4.3 Generator cost coefficients in case 4.2

Bus No.	Real power output limit (MW)		Cost Coefficients		
	Min	Max	a	b	c
1	50	140	0.00500	0.70	55
	140	200	0.00750	1.05	82.5
2	20	55	0.01000	0.30	40
	55	80	0.02000	0.60	80

Table 4.4 Comparison of the total generator fuel costs for case 4.2

Algorithm	Fuel Cost ($/hr.)				Average computational time (minutes)
	Best cost	Average cost	Worst cost	S.D. of cost	
EP [14]	650.206	654.501	657.120	2.262	69.865
TS [14]	651.246	654.087	658.911	2.054	88.447
TS/SA [14]	654.378	658.234	662.616	2.788	73.243
ITS [14]	654.874	664.473	675.035	6.888	94.832
IEP [14]	649.312	650.217	651.125	0.555	100.427
SADE_ALM	647.833	648.159	650.049	0.680	17.505
pSADE_ALM	647.833	647.833	647.833	0.000	21.568

Note: Based on differentent computing hardwares

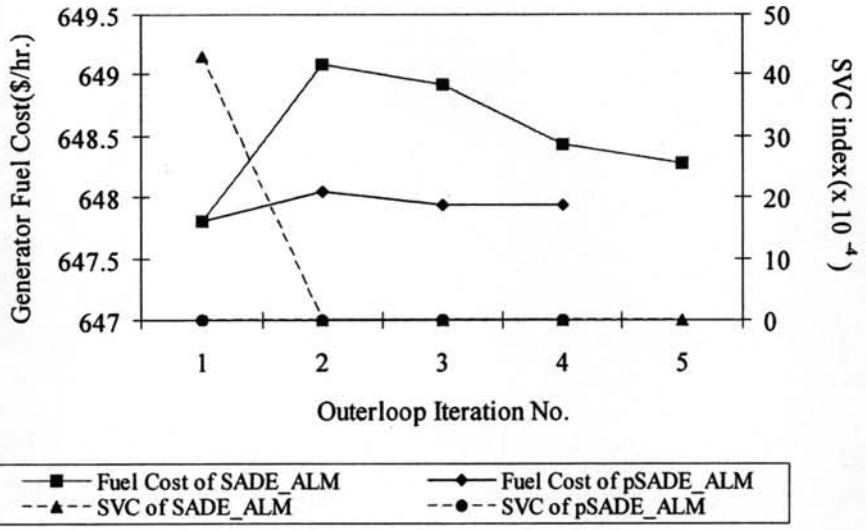

Figure 4.6 Convergence characteristic of SADE_ALM for case 4.2

4.5.3 Case 4.3: The OPF problem with valve-point effects for the IEEE 30 Bus System.

In this case, the generator fuel cost curves of generator at bus 1 and 2 are represented by quadratic functions with rectified sine components using (3.2). As in case 2, bus 5 is selected to be the slack bus of the system. The generator cost coefficients of those two generators are given in Table 4.5 [7, 14]. The simulation results are shown in Table 4.6 and the convergence characteristic of SADE_ALM and pSADE_ALM is shown in Figure 4.7.

Table 4.5 Generator cost coefficients in case 4.3

Bus No.	Real power output limit (MW)		Cost Coefficients				
	Min	Max	a	b	c	d	e
1	50	200	0.00160	2.00	150	50	0.063
2	20	80	0.01000	2.50	25	40	0.098

Table 4.6 Comparison of the total generator fuel costs for case 4.3

Algorithm	Fuel Cost ($/hr.)				Average computational time (minutes)
	Best cost	Average cost	Worst cost	S.D. of cost	
EP [14]	955.508	957.709	959.379	1.084	61.419
TS [14]	956.498	958.456	960.261	1.070	88.210
TS/SA [14]	959.563	962.889	966.023	2.146	65.109
ITS [14]	969.109	977.170	985.533	6.191	85.138
IEP [14]	953.573	956.460	958.263	1.720	93.583
SADE_ALM	944.031	954.800	964.794	5.371	16.160
pSADE_ALM	953.516	953.516	953.516	0.000	29.372

Note: Based on differentent computing hardwares

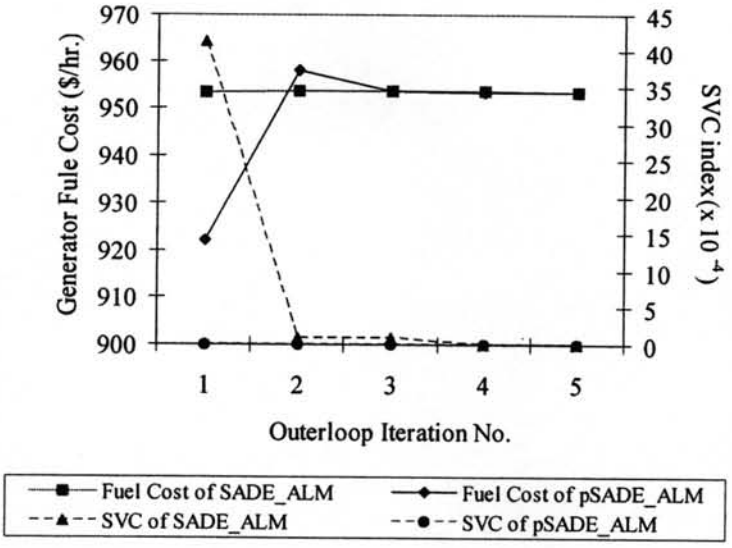

Figure 4.7 Convergence characteristic of SADE_ALM and pSADE_ALM for case 4.3

4.5.4 Case 4.4: The OPF with Combined Quadratic, Multiple Fuels, Valve-Point Effects, and Combined Cycle Cogeneration Plant (CCCP) Model for the IEEE 30 Bus System.

In this case, the first generator is assumed to be combined cycle cogeneration plant (CCCP), second generator has multiple-fuel options, and third and fourth generators have valve-point effects. For the rest of the generators, the fuel cost functions are represented by simple quadratic functions. As in case 4.2, bus 13 is selected to be the slack bus of the system. The generator cost coefficients with ramp rate data are given in Table 4.7 [12]. The simulation results are shown in Table 4.8 and the convergence characteristic of SADE_ALM is shown in Figure 4.8.

Table 4.7 Generator cost coefficients in case 4.4

Gen. No.	Bus No.	Real power output limit (MW)		Cost Coefficients						Ramp Rate Data (MW)		
		Min	Max	a	b	c	d	e	K	$P_{G_i}^0$	UR_i	DR_i
1	1	50	63.750	0	2.426	-11.95	0	0	0	135	65	85
		63.750	82.875	0	0.000	0	0	0	142			
		82.875	93.750	0	7.146	-449.5	0	0	0			
		93.750	157.500	0	2.942	-55.36	0	0	0			
		157.500	176.625	0	0.000	0	0	0	408			
		176.625	200	0	6.074	-664.9	0	0	0			
2	2	43	53	0.010	0.300	35	0	0	0	65	12	22
		53	77	0.020	0.600	60	0	0	0			
3	5	20	47	0.070	0.095	45	40	0.08	0	35	12	15
4	8	10	33	0.090	0.025	30	30	0.09	0	25	8	16
5	11	11	26	0.025	3.000	0	0	0	0	20	6	9
6	13	14	38	0.025	3.000	0	0	0	0	30	8	16

Table 4.8 Comparison of the total generator fuel costs for case 4.4

Algorithm	Fuel Cost ($/hr.)				Average computational time (minutes)
	Best cost	Average cost	Worst cost	S.D. of cost	
EP [12]	747.300	N/A	N/A	N/A	N/A
SADE_ALM	716.003	716.213	716.752	0.312	17.577
pSADE_ALM	716.021	716.021	716.021	0.000	21.851

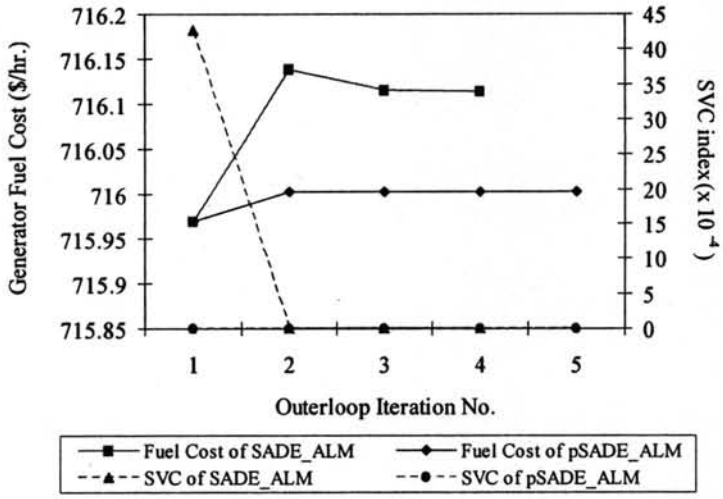

Figure 4.8 Convergence characteristic of SADE_ALM and pSADE_ALM for case 4.4

4.5.5 Case 4.5: The OPF with Quadratic Fuel Cost Function Based on the IEEE 57 and 118 Bus System.

For this case, bus 1 and 69 are the slack bus of the IEEE 57 and 118 bus system respectively. The generator cost curves of all the generators are represented by quadratic function as shown in (3.1). The generator cost coefficients for the IEEE 57 and 118 bus system are given in Table E.4 and F.4 in Appendix E and F respectively [66]. The simulation results are shown in Table 4.9 and the convergence characteristic of SADE_ALM and pSADE_ALM for both systems are shown in Figure 4.9 and 4.10.

Table 4.9 Comparison of the total generator fuel costs for case 4.5

Test System	Algorithm	Fuel Cost ($/hr.)				Average computational time (minutes)
		Best cost	Average cost	Worst cost	S.D. of cost	
57 Bus	SADE_ALM	41795.508	42348.726	43931.655	636.666	10.639
	pSADE_ALM	41710.286	41710.286	41710.286	0.001	45.918
118 Bus	SADE_ALM	142453.920	151941.503	161703.515	5973.669	23.461
	pSADE_ALM	130383.237	130383.237	130383.237	0.003	108.482

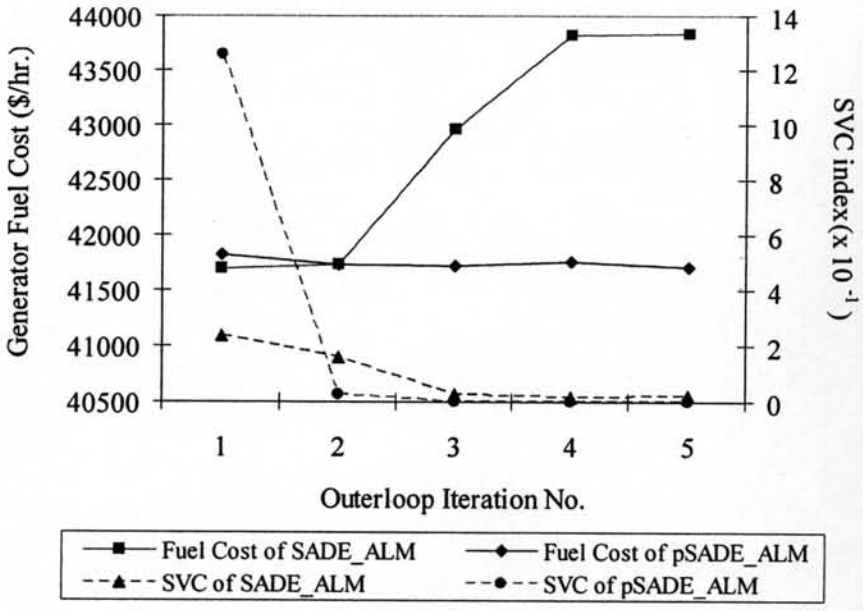

Figure 4.9 Convergence characteristic of SADE_ALM and pSADE_ALM for case 4.5 (the IEEE 57 bus system)

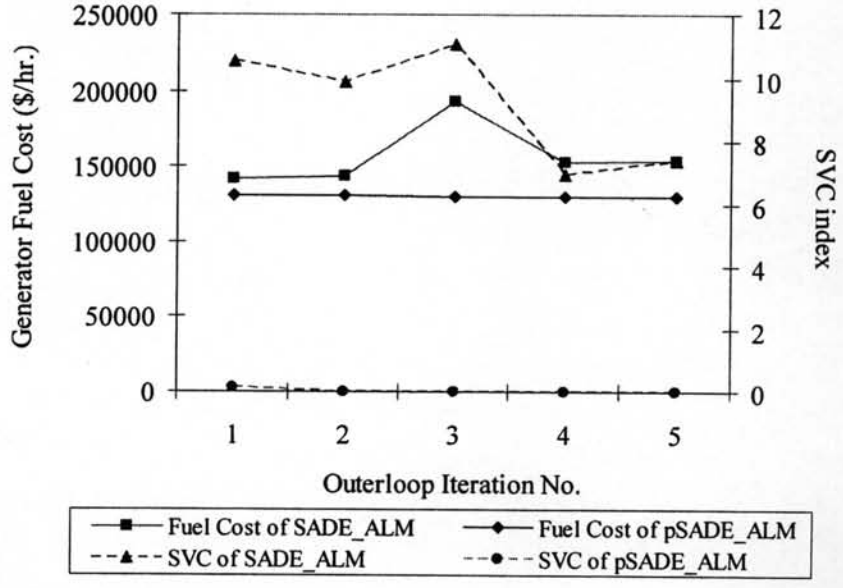

Figure 4.10 Convergence characteristic of SADE_ALM and pSADE_ALM for case 4.5 (the IEEE 118 bus system)

Based on the IEEE 30 bus system, numerical results of cases 4.1-4.4 for both SADE_ALM and pSADE_ALM from ten test runs do not violate any constraints. Tables 4.2, 4.4, 4.6, and 4.8 show that the best and the average fuel costs of both algorithms are lower than those obtained by TS, TS/SA, ITS, EP, IEP, and parallel EP except gradient base method [65] in case 4.1 where the optimal solution is very similar. In addition, for case 4.2, the best generator fuel cost of EP reported by J. Yuryevich et.al. [7] is $647.79/hr, which is less expensive than SADE_ALM in Table 4.4. However, the given solution violates reactive power of generator at bus 1, 8, and 13 by -229.59%, +20%, and -86.67% respectively. For case 4.3, the best generator fuel cost of EP, and TS reported by J. Yuryevich et.al [7], and M.A. Abido [9] respectively also are less expensive than SADE_ALM in Table 4.6. However, the best solution given in J. Yuryevich et.al [7] ($919.89/hr.) violates reactive power of generator at bus 1 by -252.04 %, and line loading 1-2 by +17%. Finally, the best solution given in M. A. Abido [9] ($919.715/hr.) also has the violation on the limit of line loading 1-2 by +4.1%.

Comparing between SADE_ALM and pSADE_ALM, we can see that the best generator fuel costs of pSADE_ALM for case 4.1, 4.2, and 4.4 are similar with SADE_ALM, whereas the best generator fuel costs of pSADE_ALM are expensive than SADE_ALM in case 4.3. However, the average, the worst and the S.D. of generator fuel costs of pSADE_ALM for case 4.1-4.4 are better than SADE_ALM as shown in Tables 4.2, 4.4, 4.6, and 4.8 respectively. These show that the robustness or the consistency of the optimal solutions determined from pSADE_ALM are better than SADE_ALM. The optimal values of the best solution given by SADE_ALM and pSADE_ALM in case 1-4 are shown in Table 4.10. Tables D.4-D.11 in Appendix D show power flow results of SADE_ALM and pSADE_ALM based on the associated best optimal solution for each case.

Based on the same parameter setting, numerical result for case 4.5 reveals that the best, the average, the worst, and the S.D. of generator fuel costs of pSADE_ALM are less expensive than SADE_ALM for 57 and 118 bus systems as shown in Table 4.9. In addition, for all ten test runs, pSADE_ALM provides the same optimal solution for all trial runs without violating any constraints, whereas SADE_ALM violates constraints slightly in trial no. 1, 3, 4, 7, and 8 for 57 bus system, and all trials for 118 bus system as shown in Table 4.11. This emphasis the pSADE_ALM is better than SADE_ALM for higher test systems.

The optimal values of the best solution given by SADE_ALM and pSADE_ALM for 57 and 118 bus system are shown in Table E.5 and F.5 in Appendix E and F respectively. In addition, Tables E.6-E.7 and F.6-F.7 in Appendix E and F show power flow results of SADE_ALM and pSADE_ALM based on the associated best optimal solution for 57 and 118 bus system respectively.

Table 4.10 The best optimal solutions given by SADE_ALM and pSADE_ALM in case 4.1-4.4

Optimal Solution	Case 1		Case 2		Case 3		Case 4	
	SADE_ ALM	pSADE_ ALM	SADE_ ALM	pSADE_ ALM	SADE_ ALM	pSADE_ ALM	SADE_ ALM	pSADE_ ALM
P_{G1} (MW)	176.1522	176.0940	140.0000	140.0000	193.2903	149.7331	176.6250	176.6250
P_{G2} (MW)	48.8391	48.8401	55.0000	55.0000	52.5735	52.0571	53.0000	52.9999
P_{G5} (MW)	21.5144	21.4981	24.1986	24.2086	17.5458	23.2772	20.0000	20.0000
P_{G8} (MW)	22.1299	22.1855	35.0000	35.0000	10.0000	34.0310	10.0000	10.0001
P_{G11} (MW)	12.2435	12.2571	18.6439	18.5943	10.0000	16.4249	17.3733	17.4531
P_{G13} (MW)	12.0000	12.0000	17.6397	17.6797	12.0000	15.5025	16.2304	16.1540
V_{G1} (p.u.)	1.0500	1.0500	1.0500	1.0500	1.0493	1.0500	1.0500	1.0500
V_{G2} (p.u.)	1.0381	1.0379	1.0402	1.0404	1.0271	1.0396	1.0386	1.0386
V_{G5} (p.u.)	1.0112	1.0108	1.0146	1.0150	1.0081	1.0138	1.0110	1.0111
V_{G8} (p.u.)	1.0190	1.0190	1.0255	1.0257	1.0109	1.0242	1.0179	1.0177
V_{G11} (p.u.)	1.0911	1.0961	1.0910	1.0907	1.0732	1.0919	1.0954	1.0856
V_{G13} (p.u.)	1.0891	1.0903	1.0821	1.0840	0.9634	1.0848	1.0876	1.1000
t_{11}	1.0556	1.0099	1.0475	1.0237	0.9612	1.0271	1.0576	0.9940
t_{12}	0.9000	0.9534	0.9139	0.9392	1.0680	0.9353	0.9039	0.9744
t_{15}	1.0070	1.0093	1.0004	1.0040	1.0118	1.0034	1.0058	1.0275
t_{36}	0.9420	0.9423	0.9451	0.9465	0.9041	0.9450	0.9419	0.9420
Fuel Costs ($/hr.)	802.404	802.405	647.833	647.833	944.031	953.516	716.003	716.021

Table 4.11 Optimal results for the IEEE 57 and 118 bus system given by SADE_ALM and pSADE_ALM for each trial run in case 4.5

Trial No.	IEEE 57 bus system				IEEE 118 bus system			
	SADE_ALM		pSADE_ALM		SADE_ALM		pSADE_ALM	
	Fuel Cost ($/hr.)	SVC index	Fuel Cost ($/hr.)	SVC index	Fuel Cost ($/hr.)	SVC index	Fuel Cost ($/hr.)	SVC index
1	42671.820	0.0137	41710.286	0	149951.870	7.6540	130383.237	0
2	41795.508	0.0000	41710.286	0	142453.920	1.1131	130383.237	0
3	42012.763	0.0115	41710.286	0	161703.515	4.7328	130383.237	0
4	42641.993	0.0001	41710.286	0	150446.156	8.7776	130383.237	0
5	42023.418	0.0000	41710.286	0	148625.163	4.5063	130383.237	0
6	42345.237	0.0000	41710.286	0	147477.105	5.2237	130383.237	0
7	42287.809	0.0008	41710.286	0	153852.693	4.0102	130383.237	0
8	41888.548	0.0115	41710.286	0	148405.675	10.4295	130383.237	0
9	43931.655	0.0000	41710.286	0	159472.628	4.2020	130383.237	0
10	41888.507	0.0000	41710.286	0	157026.301	2.9650	130383.237	0

4.6 Conclusion

The sequential self-adaptive differential evolution with augmented lagrange multiplier method (SADE_ALM) and parallel SADE_ALM called pSADE_ALM were applied to solve the OPF problems for generators with non-smooth and nonconvex fuel cost functions. The effectiveness of both algorithms have been tested on the IEEE 30-bus system with different fuel cost characteristics. Numerical results show that the sequential SADE_ALM is successfully and effectively implemented to find the best total generator fuel cost of the OPF problems compared with other approaches, i.e. tabu search (TS), hybrid tabu search and simulated annealing (TS/SA), improved tabu search (ITS), evolutionary programming (EP), improved evolutionary programming (IEP), parallel EP, and pSADE_ALM. However, for higher test system, i.e. 57 and 118 bus system, the pSADE_ALM provide the best generator fuel cost less expensive than SADE_ALM without violating any constraints. In addition, the robustness of the optimal results determined from each trial for all test cases of pSADE_ALM is significantly better than SADE_ALM. Therefore, the pSADE_ALM shows promising capability for solving the OPF problems especially in larger system. However, the average computational time of pSADE_ALM for all test cases is higher than SADE_ALM. The main reason for this is that there is the bottle neck at the inner loop iteration of pSADE_ALM. The computational time for inner loop iteration of pSADE_ALM are higher than SADE_ALM since the master node has to wait the elite members from every nodes including the master node before proceeding the outer loop iteration, whereas the SADE_ALM can proceed the outerloop iteration immediately without idle time. This drawback is still needed to be improved for future research.

In the next chapter, we will discuss the solution procedure of the security constrained optimal power flow (SCOPF) using both sequential and parallel algorithm of SADE_ALM, since the primary limitation of the OPF solution is lack of system security or contingency constraints pertaining to credible outages of transmission lines and/or generating plants. Security of the system requires that the optimal operation of the system is not only feasible for the intact system (N-0) but also for the contingency cases (N-1). Therefore, in order to ensure security of the system, contingency constraints for a few severe contingencies should be identified and OPF schedule should be corrective rescheduling to eliminate limit violation.